Development of an Antilock Brake System for Electric Vehicles Without Wheel Slip and Road Friction Information

Kyoungseok Han, Byunghwan Lee, and Seibum B. Choi, *Member, IEEE*

***Abstract*—This paper presents a control method of an antilock brake system (ABS) for electric vehicles. For decades, serious efforts have been dedicated to designing a wheel slip-based ABS controller, but there are some inherent flaws. To realize a robust control system, the wheel slip and road friction information are generally required. Unfortunately, however, these parameters cannot be accurately measured in production vehicles. The method suggested in this paper is aimed at solving these problems by exploiting the nonlinear characteristics of tire force. The optimal wheel slip can thereby be found without wheel slip and road friction information. We employ the motor as an actuator instead of a conventional hydraulic brake system at the front wheels. However, the rear wheels are still hydraulically controlled. That is, the front and rear wheels have different roles in the proposed method. This hardware configuration can be changed for control purposes, so the proposed approach is not designed for a specific hardware configuration. The performance of the proposed method is confirmed by simulations and real vehicle-based experiments.**

***Index Terms*—Antilock brake system (ABS), wheel slip control, sliding mode control, electric vehicles, in-wheel motors.**

I. Introduction

The antilock brake system (ABS) is a representative technology for longitudinal vehicle dynamics control systems. The primary function of the ABS is to prevent excessive or insufficient wheel slip, meaning that the vehicle can decelerate with maximum braking while maintaining the vehicle's steerability [1]. To achieve this objective, appropriate wheel slip control should be established, taking into account the given road friction information that determines the physically available maximum deceleration of the vehicle.

Manuscript received June 30, 2018; revised December 11, 2018 and March 14, 2019; accepted April 8, 2019. Date of publication April 17, 2019; date of current version June 18, 2019. This work was supported in part by Hyundai Motor Company, in part by the National Research Foundation of Korea (NRF) funded by the Korean government (MSIP) under Grant 2017R1A2B4004116, and in part by the BK21+ program through the NRF funded by the Ministry of Education of Korea. The review of this paper was coordinated by Prof. T. Shim. *(Corresponding author: Seibum B. Choi.)*

K. Han is with the University of Michigan, Ann Arbor, MI 48109 USA (e-mail: kyoungsh@umich.edu).

B. Lee is with the Hyundai Motors Group, Uiwang-si 437-815, South Korea (e-mail: bhlee1060@hyundai.com).

S. B. Choi is with the Korea Advanced Institute of Science and Technology, Daejeon 305-806, South Korea (e-mail: sbchoi@kaist.ac.kr).

Digital Object Identifier 10.1109/TVT.2019.2911687

A. Literature Review

The numerous attempts to obtain road friction information in real-time have been made by many researchers [2]–[8], but their performance has not reached a satisfactory level.

In addition, the wheel slip determined from vehicle and wheel speed information is very inaccurate in production vehicles, but implementing a wheel slip-based ABS algorithm requires accurate wheel slip information. Although there have been many literature which attempted to estimate the wheel slip based on measured longitudinal acceleration, the drift and offset of the estimated values were inevitable [2], [3].

To summarize, these two inaccurate vehicle and/or tire parameters, i.e., road friction and wheel slip, are the main obstacles for preventing wheel slip-based control.

In order to overcome these technical shortcomings, the ABS controllers developed for production vehicles are usually designed based on a rule-based algorithm, which requires heavy computational burden and limits the control performance for safety reasons [1]. Therefore, the widely adopted ABS algorithms in production vehicles are not designed to track the optimum wheel slip point where maximum braking force is generated. Instead, most of the mass production systems empirically determine the reference wheel slip. This is done by considering the wheel acceleration in a control loop and a set of corresponding rules. It is normally activated when one of the four wheels decreases rapidly. The reduced wheel speed is recovered at the appropriate speed by controlling the hydraulic valves in the brake systems. Since the appropriate speed does not imply an optimal speed, robust wheel slip-based control that tracks the optimal wheel speed, not a rule-based method, has a potential to significantly improve the control performance in production ABS.

However, as mentioned earlier, there are two main difficulties in implementing a wheel slip-based control. First, the desired wheel slip, which varies significantly depending on road friction, is not explicitly given in actual driving [9], [10]. Because the road friction information cannot be estimated accurately, the desired wheel slip is also not easily defined. That is, the desired value that the state variable of the control system should track is not clearly defined. Further exacerbating the situation, the current state variable (real-time wheel slip) is also very inaccurate in production vehicles, which is a second challenging issue. In summary, unlike the conventional control situations, when designing ABS, neither the desired value nor current value is given. This is why the rule-based algorithms are widely accepted in automotive manufacturing.

Many previous studies have attempted to improve the wheel slip-based ABS control performance. However, the following drawbacks need to be further researched to increase the feasibility.

Most of the previous methods assumed that the desired wheel slip has been given in advance [11]–[14], which can also be interpreted to mean that road friction information is available in real-time. However, as mentioned, this is not always possible. In [15], a practical ABS control algorithm is presented under the assumptions that wheel slip is not being measurable, and optimal slip is not also given. However, the algorithm should be verified with more accurate models to consider the real driving. In addition, some studies using the quarter car model [16], [17] do not consider the dynamic weight shifting effect, which significantly influences the control performance. That is, actual vehicle-based experimental validation has often been replaced by simulation or simplified hardware-in-the-loop (HIL) testing. However, in general, the simulation results are very different from actual experimental results of production vehicles. Therefore, the algorithm development process should be combined with numerous experiments to consider practical issues that cannot be explained by general mathematical principles. In this way, the robustness of the developed algorithms can be improved. Although the developed wheel slip algorithm is verified using experimental vehicle, the used actuators are over specification for mass production considering cost competitive [18], [19].

B. Research Contribution

This paper focuses on practical aspects. The developed algorithm does not require road friction information and current wheel slip. We use the nonlinear characteristics of the tire force to overcome the insufficient amount of information mentioned above. The wheel slips were controlled based on the monitored signs of the time derivative of two major state variables. This was possible due to the special structure of the sliding mode controller that is used.

In addition, the front and rear wheels play different roles. Using the fast dynamics of the motors, the front wheels continue to find the optimal wheel slip point and real time front wheel speed is defined as the desired wheel speed. At the same time, the rear wheels are controlled to track the desired wheel speed defined from the control results of the front wheels. This is a central part of the proposed method. To verify the robustness of the developed method, simulations and real vehicle-based experiments were conducted and the results demonstrated its feasibility. Also, the test vehicle is identical to the commercially available vehicle, and the specification of the actuator is appropriate for mass production.

C. Paper Organization

The remainder of this paper is organized as follows. In Section II, we discuss the well-known problems of the conventional ABS and present an overview of the proposed method. The detailed design process of the controller is shown in Section III. We present simulation and experimental results in Sections IV and V, and conclude the paper in Section VI.

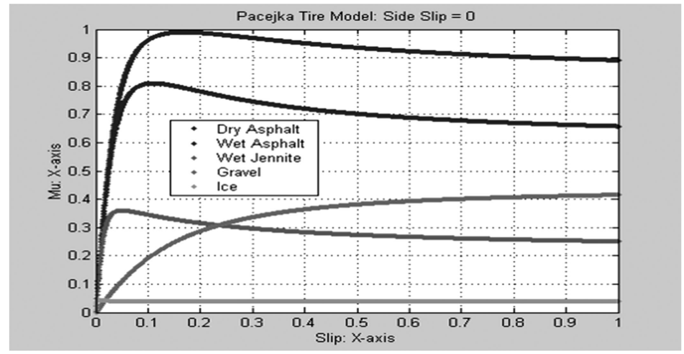

Fig. 1. Tire friction-slip curves based on Pacejka Tire Model.

II. Conventional ABS and Overview of Proposed Method

Before introducing the developed control method, technical shortcomings of the conventional ABS are reviewed in this section. In addition, the main considerations of this paper are overviewed.

A. Technical Shortcomings of Conventional ABS

The wheel slip during braking is defined as follows:

$$\lambda = \frac{r_e \omega - V_{car}}{V_{car}}. \quad (1)$$

where r_e is the effective wheel radius, ω is the wheel angular speed, and V_{car} is the absolute vehicle speed.

As mentioned earlier, V_{car} is not provided in real-time on a production vehicle and r_e is also not always constant. Therefore, the current wheel slip λ cannot be measured accurately. In addition, the friction curve of Fig. 1 which is formulated based on Pacejka tire model [20] depicts that the optimal slip point λ_d that gives the maximum friction force varies significantly depending on the road surfaces. Unfortunately, this maximum friction force, i.e., road friction, is not provided in the real world, which means that the vehicle should be controlled without road friction and wheel slip information.

If λ_d and λ are provided in actual driving, a cost function *J* to be minimized is defined as follows:

$$\arg\min_{u} J = f\left(\|\lambda - \lambda_d\|_n\right). \quad (2)$$

Here, *u* is the control input such as motor and/or brake torque.

The control performance will not be substantially different regardless of the controller type if the cost function of (2) is well defined. However, this is a challenging task, as described above, and thus adopting an ABS controller that relies solely on wheel slip information should be avoided for safety reasons.

In addition, even if a cost function *J* is well defined, there is still a major problem to be solved. The dynamic response of the actuator is an important factor that determines the control

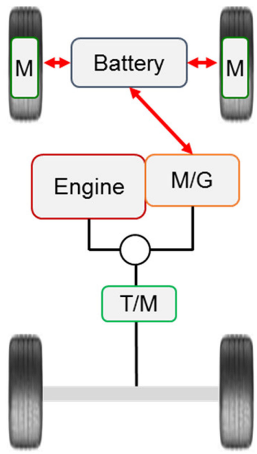

Fig. 2. Electric powertrain architecture of the target vehicle.

performance. In general, a low control actuation time delay and high actuator bandwidth are desired to ensure satisfactory performance. Therefore, in this paper, a motor that generally has a fast-dynamic response is employed as an actuator at the front wheels. In addition, hydraulic brake system is also used to control the system in a wide range of areas at the rear wheels. The electric powertrain architecture of the target vehicle will be discussed in the next section.

B. Overview of Proposed Method

We aim to design a robust ABS controller without wheel slip and road friction information. The main difference between the conventional and proposed approach is that the hydraulic brake and the regenerative brake are integrated to take advantage of each actuator. Using the fast-dynamic characteristics of the motor, the front wheels are used to find the reference value. Correspondingly, the rear wheel tracks the defined reference by controlling the hydraulic brake system.

To increase the feasibility, the proposed method is developed with consideration of the following factors:

(i) Only measurable sensor signals in the production vehicles are used when designing the controller.
(ii) The motors used as the actuators are assumed to have a dynamic response that is fast enough to find the optimal wheel slip point.
(iii) The estimation processes required at intermediate steps such as vehicle and tire model parameters are minimized.

With the above-mentioned points in mind, we present a robust wheel-slip based ABS controller and conduct numerous simulations and experiments to verify the developed algorithm.

III. Controller Design

A. Description of Powertrain Architecture

Fig. 2 describes the electric powertrain architecture of the target vehicle. This is a type of parallel hybrid systems, but the main distinction is that additional in-wheel motors (IWMs) are employed at the front wheels. Basically, the target vehicle is

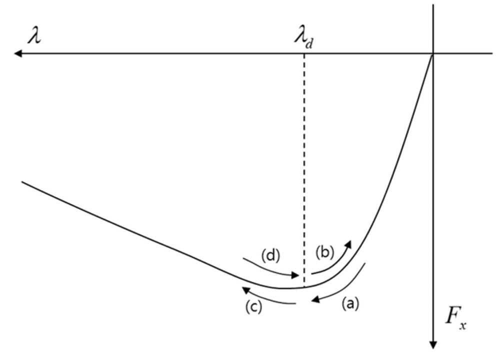

Fig. 3. Nonlinear tire force curve, and the behaviors of tire force and slip near the optimal slip point.

rear wheel drive, but a part-time four wheel drive system can be realized by operating IWMs. Due to this particular powertrain configuration, we can propose a new control method.

Because the IWM's response is much faster than that of a conventional hydraulic system [21], [22], the front wheels are suitable for finding the optimal wheel speed for maximum vehicle deceleration. We denote this process the cycling control, and details of the process are discussed in the next sub-section. The rear wheels are controlled by the conventional hydraulic brake, and they track the defined speed from control results of the front wheels. By adopting this cycling control, the need for defining cost function in (2) can be eliminated in the entire algorithm.

B. Dynamic Model of the Wheel

The rotational dynamics for the wheel during braking is expressed as follows:

$$J_w \dot{\omega}_{f/r} = r_e F_{x,f/r} - T_{b,f/r} + \alpha, \tag{3}$$

where J_w is the wheel inertia, $F_{x,f/r}$ is the front/rear tire force, $T_{b,f/r}$ is the brake torque, and $\alpha \ll 1$ is the negligible uncertainties, such as aero effect and rolling resistance.

Since the front and rear wheels are controlled using the different actuators, $T_{b,f/r}$ is defined as follows:

$$T_{bf} = K_t i_m = \eta_r T_{b,t}, \tag{4}$$

$$T_{br} = \kappa_r P_{mc} = (1 - \eta_r) T_{b,t}. \tag{5}$$

where K_t is the motor constant, i_m is the current passing through the motor, κ_r is the brake gain for the rear wheels, P_{mc} is the pressure of the master cylinder, $T_{b,t}$ is the total brake torque and η_r is the brake torque distribution ratio where $0 < \eta_r < 1$.

C. Nonlinearity of Tire

As shown in Fig. 3, the longitudinal tire force varies depending on the wheel slip, and maintaining the current wheel slip λ at the optimal slip point λ_d is the ultimate goal of ABS. As mentioned, if both λ and λ_d are given in real-time, the goal of ABS can be easily achieved, but this practical issue is challenge, which prevents the introduction of slip-based ABS.

TABLE I
THE SIGNS OF THE TIME DERIVATIVE OF TIRE FORCE AND WHEEL SLIP

Areas	$\mathrm{sgn}(\dot{F}_x)$	$\mathrm{sgn}(\dot{\lambda})$	$\mathrm{sgn}(\dot{F}_x \cdot \dot{\lambda})$
(a)	-	-	+
(b)	+	+	+
(c)	+	-	-
(d)	-	+	-

The time derivative of (1) is as follows:

$$\dot{\lambda} = \underbrace{\frac{r_e}{V_{car}}\dot{w}}_{(a)} - \underbrace{\frac{r_e w}{V_{car}^2}a_x}_{(b)}, \tag{6}$$

where a_x is the acceleration of the vehicle.

Since the rotational motion of the wheel oscillates significantly when the ABS operates, the magnitude of $\dot{\lambda}$ is mainly determined by (a) in (6). Therefore, the sign of $\dot{\lambda}$ near the optimal slip λ_d is approximated as follows:

$$\mathrm{sgn}(\dot{\lambda}) \approx \mathrm{sgn}(\dot{w}), \tag{7}$$

This is because V_{car} and r_e are always positive. As seen from Fig. 3, F_x begins to decrease when the current wheel slip λ passes through λ_d. Therefore, the $\mathrm{sgn}(\dot{F}_x)$ changes at this point.

Based on these relationships, the following is derived:

$$\mathrm{sgn}(\lambda - \lambda_d) \approx \mathrm{sgn}(\dot{F}_x \cdot \dot{w}), \tag{8}$$

Although the magnitude of $(\lambda - \lambda_d)$, which is generally used as a cost function in conventional wheel slip-based ABS (2), is difficult to determine, at least its sign can be determined based on (8) near the optimum wheel slip point.

Table I depicts the signs of $\dot{\lambda}$, $\dot{F}_x$, and their products. Our approach relies on the fact that $\mathrm{sgn}(\dot{F}_x, \cdot\dot{w})$ has a different sign based on the optimal wheel slip point, λ_d. We present a cycling control method using this relationship.

D. Tire Force and Wheel Speed Observers

As described in the previous sub-section, the $\mathrm{sgn}(\lambda - \lambda_d)$ can be derived from (8). In production vehicles, *w* can be measured quite accurately when the wheel speed is above 10 km/h. However, the time derivative of *w* is easily contaminated by noise, which can provide an incorrect sign of $\dot{w}$. In addition, the tire force F_x is not given in production vehicles. Therefore, tire force and wheel speed observers are designed.

This paper adopts the wheel speed and tire force estimation strategy in [10], [23], [24] as follows:

$$\dot{\hat{\omega}}_f = \frac{r_e}{J_w}\hat{F}_{xf} - \frac{1}{J_w}T_{bf} + l_1\left(\omega_f - \hat{\omega}_f\right), \tag{9}$$

$$\dot{\hat{F}}_{xf} = l_2\left(\omega_f - \hat{\omega}_f\right), \tag{10}$$

where l_1 and l_2 are the non-negative gains and their magnitudes are determined by considering the physical estimation error bounds, as in our previous work [10]. Also, the stability of the designed observers is analyzed as in [10].

Since the constructed observers in (9) and (10) are strongly related to each other, $\mathrm{sgn}(\dot{F}_x, \cdot\dot{w})$ is consistent. In addition, contaminated measurement in *w* by noise is filtered out by the feedback term. Based on this, $\mathrm{sgn}(\lambda - \lambda_d)$ can be assumed as $\mathrm{sgn}(\dot{F}_x, \cdot\dot{w})$ near the optimal slip point.

E. Front Wheel Cycling Control

As mentioned earlier, the IWMs at the front wheels are used to find the optimum slip point. When the magnitude of the front tire slip exceeds the desired slip point ($|\lambda| \geq |\lambda_d|$), the IWM is controlled to reduce the exerted torque.

The switching surface is generally defined as follows:

$$s_1 = \lambda_f - \lambda_{fd}, \tag{11}$$

The control objective is to make *s* converge to zero. This can be achieved by defining a control law including feed-forward and feedback term.

In order to demonstrate the overall stability of the observer and controller, the following Lyapunov function candidate is defined:

$$V = \frac{1}{2}s_1^2 + \frac{1}{2}e^2, \tag{12}$$

where $\mathrm{e} = \omega_f - \hat{\omega}_f$.

The time derivative of (12) is calculated as follows:

$$\dot{V} = s_1\left(\dot{\lambda}_f - \dot{\lambda}_{fd}\right) + e\left(\dot{\omega}_f - \dot{\hat{\omega}}_f\right), \tag{13}$$

Substituting (3), (6), and (9) into (13) results in,

$$\dot{V} = s_1\left(\frac{r_e}{V_{car}}\dot{w}_f\right) + e\left(\frac{r_e}{J_w}\tilde{F}_{xf} - l_1 e\right), \tag{14}$$

In (14), $\dot{\lambda}_{fd}$ is assumed to be zero because a homogeneous road surface is considered in this paper, and $\tilde{F}_{xf} = F_{xf} - \hat{F}_{xf}$. In addition, only (a) of (6) is considered since the region near the optimal slip point is the area of interest.

Subsequently, (14) can be manipulated by considering wheel dynamics model as follows:

$$\dot{V} = s_1\left\{\frac{r_e}{V_{car}}\left(\frac{r_e}{J_w}F_{xf} - \frac{1}{J_w}T_{bf}\right)\right\} + e\left(\frac{r_e}{J_w}\tilde{F}_{xf} - l_1 e\right), \tag{15}$$

The control law is defined as follows:

$$u = T_{bf} = r_e\hat{F}_{xf} + \eta\frac{J_w V_{car}}{r_e}\mathrm{sgn}(s_1), \tag{16}$$

where η is the positive control gain and $\hat{F}_{xf}$ is determined from the constructed observer.

To ensure the asymptotic stability of (15), the following condition is satisfied:

$$\dot{V} < 0 \text{ for } s_1 \neq 0. \tag{17}$$

Substituting (16) into (15) leads to:

$$\dot{V} = -\eta \cdot s_1 \cdot \mathrm{sgn}(s_1) - l_1 e^2 - \frac{r_e\tilde{F}_{xf}}{J_w e}\left(\frac{r_e e}{V_{car}}s_1 - e^2\right), \tag{18}$$

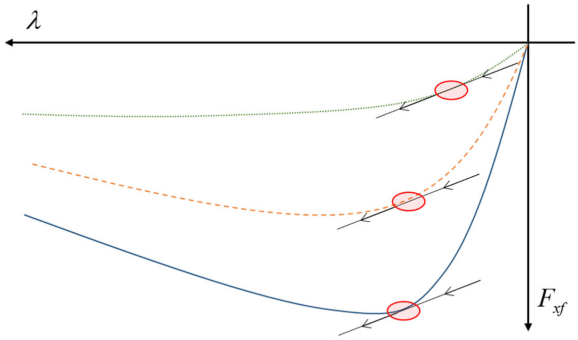

Fig. 4. The relationship between tire force and wheel slip on different road surfaces.

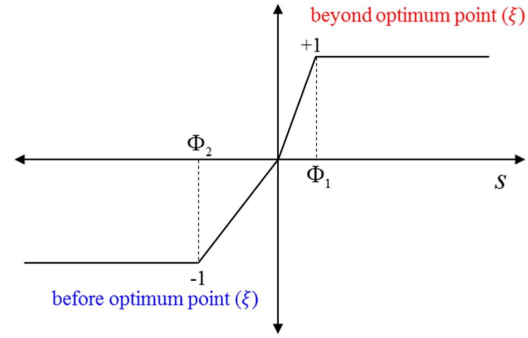

Fig. 5. Saturation function with asymmetrical smoothing factors.

Equation (18) satisfies the stability condition of (17) by Barbalat's lemma [25] if the control gain (η) and observer gain (l_1) are defined as follows:

$$l_1 > C_{e1} \geq \left\| \frac{r_e \tilde{F}_{xf}}{J_w e} \right\|_1, \tag{19}$$

$$\eta > C_{e2} \geq \left\| \frac{\tilde{F}_{xf} r_e^2}{J_w V_{car}} \right\|_1. \tag{20}$$

where C_{e1} and C_{e2} are the positive constants, and they can be determined by considering physical bounds of magnitudes of the estimation errors [26], i.e., $\tilde{F}_{xf}$ and e.

Thus far, the conventional sliding model controller has been designed. However, as mentioned earlier, s_1 of (16) is very difficult to estimate or measure. Therefore, the following control law that exploits the derived relationship in (8) is presented instead of (16):

$$u = T_{bf} = r_e \hat{F}_{xf} + \eta \frac{J_w V_{car}}{r_e} \operatorname{sgn}(\dot{\hat{F}}_{xf} \cdot \dot{\hat{w}}_f). \tag{21}$$

Usually, the $\operatorname{sgn}(\cdot)$ term of the sliding controller is replaced by the $\operatorname{sat}(\cdot)$ term to reduce control chattering, which is a widely known disadvantage of sliding mode control [27]. However, the suggested control law (21) instead exploits this disadvantage to find the optimal slip point. Through motor control using (21), the front wheels are controlled to cycle around the optimal point regardless of the road surface. On the basis of this method, the technical issue of the conventional ABS, i.e., unknown λ and λ_d, can be resolved theoretically.

However, due to the high sensitivities of $\dot{\hat{F}}_{xf}$ and $\dot{\hat{w}}_f$, the robustness of (21) for various types of road surfaces should be further ensured sufficiently. For example, several road surfaces, especially those with low friction, do not explicitly display the peak point at the tire force versus slip curve. Consequently, the magnitude of the absolute value of tire force increases monotonically without reduction, and (21) results in locking up of the wheels.

As illustrated in Fig. 4, the instantaneous slip-slopes, i.e., $\partial F_{xf}/\partial \lambda$, converge to around zero regardless of the surface types, as the absolute value of wheel slip increases. If the target slip-slope ξ_d is specified with a safety margin other than zero, at least the controlled wheel will not be unstable on surfaces where the peak slip point is not explicitly expressed.

The instantaneous slip-slope near the optimal slip point can be defined as follows:

$$\xi = \frac{\partial F_{xf}}{\partial \lambda} = \frac{\partial F_{xf}}{\partial t} \cdot \frac{\partial t}{\partial \lambda} = \frac{V_{car} \dot{\hat{F}}_{xf}}{r_e \dot{\hat{w}}_f}. \tag{22}$$

We assume that the estimated state variables from the constructed observers in (9) and (10) are free from measurement noise by applying the filtering technologies. A certain level of rule-based filtering is inevitable to ensure the robustness. Therefore, (22) can be assumed to provide a fairly accurate slip-slope near the optimum point.

We present the following control law instead of (21):

$$u = T_{bf} = r_e \hat{F}_{xf} + \eta \frac{J_w V_{car}}{r_e} sat\left[(\xi - \xi_d)/\Phi_{1,2}\right]. \tag{23a}$$

For convenience, we define the sliding surface as follows:

$$s_2 = \xi - \xi_d. \tag{23b}$$

where ξ_d is the predefined desired slip-slope with a safety margin and can be determined by numerous experiments considering the vehicles type, size of the wheel, and other uncertainties.

In addition, Φ is a smoothing factor that reduces the amplitude of control chattering. As shown in Fig. 5, the smoothing factors are specified with asymmetrical values, i.e., $|\Phi_2| > |\Phi_1|$, because rapid brake torque reduction must be performed to prevent locking up of the wheels. In contrast, it is desirable to apply the brake torque slowly when approaching the optimal slip point. Also, since V_{car} cannot be measured accurately in real-time in production vehicles, V_{car} is derived from the maximum value of rear wheel speeds, i.e., $\hat{V}_{car} = f(P_{mc}) \cdot \max(r_e w_{rl}, r_e w_{rr})$. Here, *rl* and *rr* indicate the rear left and rear right tires, and $f(P_{mc}) \in [0.9,\ 1]$ is a correction factor to compensate for this speed approximation error that needs to be tuned empirically and is given as a look-up table indexed by measurable master cylinder pressure. The $f(P_{mc})$ decreases nonlinearly as P_{mc} increases. This speed approximation is effective until the rear wheel's speeds are controlled independently of the master cylinder pressure, which is a common method of the production ABS control system. However, in this paper, unlike the front wheels, the rear wheels are controlled by master cylinder pressure, so this approximation holds always. The control method for the rear wheels is introduced in the next sub-section.

Moreover, compared to the slip-based controller, the proposed approach is less sensitive to the speed approximation error defined above. Let $\hat{\lambda} = \frac{r\omega - \hat{V}_{car}}{\hat{V}_{car}}$ be the slip calculated with the approximated speed $\hat{V}_{car}$, then the difference compared to the actual slip λ is defined as follows:

$$e^{\lambda} = \frac{\lambda - \hat{\lambda}}{\lambda} = \frac{r_e \omega (\hat{V}_{car} - V_{car})}{\hat{V}_{car}(r_e \omega - V_{car})}. \tag{24}$$

Similarly, we can define the instantaneous slip-slope $\hat{\xi}$ calculated with $\hat{V}_{car}$ as,

$$\hat{\xi} = \frac{\hat{V}_{car}\dot{\hat{F}}_{xf}}{r_e \dot{\hat{w}}_f}. \tag{25}$$

The difference caused by the speed approximation error can be defined as similar to (24):

$$e^{\xi} = \frac{\xi - \hat{\xi}}{\xi} = \frac{V_{car} - \hat{V}_{car}}{V_{car}}. \tag{26}$$

Now we analyze the relative size of (24) and (26):

$$\frac{e^{\lambda}}{e^{\xi}} = \underbrace{\frac{V_{car}}{\hat{V}_{car}}}_{l} \cdot \underbrace{\frac{r_e \omega}{(V_{car} - r_e \omega)}}_{m}. \tag{27}$$

Without proof, we can conjecture the magnitude of *l* is close to one, i.e., $l \cong 1$, and $m \in \mathbb{R}_{\gg 1}$ is much larger than *l*. Therefore, the ratio between e^{λ} and e^{ξ} can be assumed as,

$$\frac{e^{\lambda}}{e^{\xi}} \gg 1 \quad \rightarrow \quad e^{\lambda} \gg e^{\xi}. \tag{28}$$

Based on (28), we can conclude that the proposed approach is much less influenced by the speed approximation error than with conventional slip-based controller.

As seen from (23a), the performance of designed control law is determined by the estimated tire force $\hat{F}_{xf}$ and wheel speed $\hat{w}_f$. Therefore, the observer gain selection is a crucial task, and we follow the strategy of previous our work in [10] where the robustness of designed observer is sufficiently verified by the simulations.

F. Continuous Slip Control for Rear Wheel

By monitoring the cycling patterns of the front wheels, the desired wheel speed could be defined in previous section. The monitored front wheel speed was smoothed using a low-pass filter and a rate limiter considering the physical constraints of the vehicle and the actuator. This is why we intentionally oscillated the front IWMs, and now the controller for the rear wheels is conventionally established as follows.

The switching surface is defined as the wheel speed error as follows:

$$s_3 = \omega_r - \omega_{rd}, \tag{29}$$

where ω_{rd} is the desired rear wheel speed defined by monitoring the cycling patterns of the IWMs.

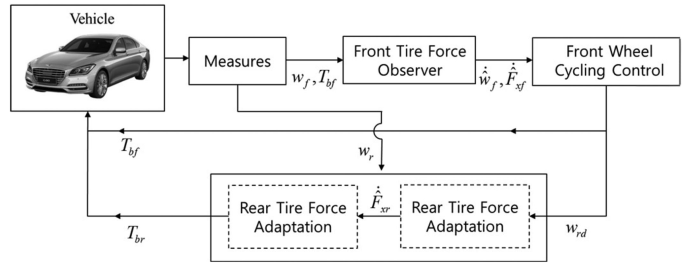

Fig. 6. Overall architecture of the proposed ABS approach.

For the asymptotic stability, the following condition should be satisfied:

$$\dot{s}_3 = -\gamma s_3, \tag{30}$$

where γ is the non-negative control gain.

Therefore, the control law for rear wheels is calculated as follows:

$$\dot{\omega}_r - \dot{\omega}_{rd} = -\gamma \left(\omega_r - \omega_{rd}\right), \tag{31a}$$

$$\frac{r_e}{J_w}F_{xr} - \frac{1}{J_w}T_{br} = \dot{\omega}_{rd} - \gamma\left(\omega_r - \omega_{rd}\right), \tag{31b}$$

Based on this, the desired rear wheel brake torque is as follows:

$$u = T_{br} = r_e \hat{F}_{xr} - J_w \dot{\omega}_{rd} + J_w \cdot \gamma \left(\omega_r - \omega_{rd}\right). \tag{31c}$$

Here, $\hat{F}_{xr}$ is assumed to be an unknown parameter that varies slowly, and hence an adaptive scheme [28] is considered.

A Lyapunov candidate function is defined as follows:

$$V = \frac{1}{2}s_3^2 + \frac{1}{2k_a}\left(F_{xr} - \hat{F}_{xr}\right)^2. \tag{32}$$

The time derivative of the above function leads to:

$$\begin{aligned}\dot{V} &= s_3\left(\frac{r_e}{J_w}\left(F_{xr} - \hat{F}_{xr}\right) - \gamma s_3\right) - \frac{1}{k_a}\left(F_{xr} - \hat{F}_{xr}\right)\dot{\hat{F}}_{xr} \\ &= -\gamma s_3^2 + \left(F_{xr} - \hat{F}_{xr}\right)\left(\frac{r_e}{J_w}s_3 - \frac{1}{k_a}\dot{\hat{F}}_{xr}\right),\end{aligned} \tag{33}$$

where k_a is the adaptation gain.

In order to satisfy (17), the adaptation law is established as follows:

$$\dot{\hat{F}}_{xr} = k_a \frac{r_e}{J_w} s_3. \tag{34}$$

Now, the feed-forward term of (31c) is constructed by the adaptation law of (34). Therefore, the established control law of (31c) can control the rear wheels to track the desired wheel speed.

G. Algorithm Overview

Fig. 6 illustrates the overall architecture of the proposed approach. Unlike conventional wheel slip-based ABS, the desired wheel slip is not given. Moreover, the current wheel slip is not measured or estimated in real-time. Instead, the estimated state variables, i.e., $\dot{\hat{w}}_f$ and $\dot{\hat{F}}_{xf}$, are used to control the front wheels. As a result, the desired wheel speed for the rear wheels can be defined by monitoring the front wheel speed profile. This is the major distinction between the conventional and proposed method. Correspondingly, the rear wheels are controlled by a hydraulic brake system using an adaptive scheme. In addition, it can be confirmed that only the sensor signals available in the production vehicle are used, which can improve the feasibility. Also, the designed controllers for the front and rear wheels work independently at the same time. In fact, from a practical standpoint, it is suggested to change the role of the front and rear wheels. Because the performance of vehicle deceleration is mainly determined by the front wheel during braking, the frequent oscillation of the front wheel may deteriorates the whole control performance. Unfortunately, since the hardware configuration was fixed and could not be changed easily.

This paper aims to propose a novel control concept for advanced ABS regardless of the hardware configuration, so the proposed method is applicable to other hardware configuration, i.e., front: hydraulic brake, rear: IWMs, both are hydraulic (conventional) or IWMs (pure electric vehicle).

IV. Simulation Results

To verify the effectiveness of the proposed method, simulations are performed using CarSim, a high-fidelity vehicle dynamics solver package.

We specified the simulation environment as follows. An E-class sedan vehicle model, provided by CarSim, is utilized, and the simulations are performed in two scenarios on the low friction surfaces. The model parameters of the vehicle are set to be the same as a luxury sedan vehicle on the market. However, to confirm the maximum achievable control performance, the shorter update time is exploited, and the controller is operated with a 5 ms sampling time that is fast enough.

The first simulation results are shown in Fig. 7, which does not consider the actuation delay. As depicted in Fig. 7(a), the front wheels are controlled by the IWMs and continuously find the optimal wheel slip. Therefore, a certain amount of oscillation on the control input (T_{bf}) is inevitable. Accordingly, the hydraulic brake control input (T_{br}) is imposed on the rear wheels to track the front wheel speed, as shown in Fig. 7(a). Note that control inputs to the rear wheels are applied at a relatively slower speed compared with those of the front wheels. This is because the dynamic responses of the actuators employed in this study are different relative to each other, and we take advantage of these characteristics.

Fig. 7(b) shows the speed trajectories of the vehicle and wheels. As expected, the vehicle decelerates while maintaining optimal wheel slip and the control performance can be assessed from the vehicle deceleration results in Fig. 7(c). Theoretically, the vehicle can decelerate up to 0.20 g because the surface friction coefficient is set to 0.20. As depicted in Fig. 7(c), the proposed method shows excellent performance until the vehicle stops. Fig. 7(d) shows the wheel slip profiles for the front and rear wheels. Since the rapid dynamic response of the IWMs is exploited, the front wheels can be controlled to cycle around the optimum slip point without under or over slip. It should be noted that the results-above are not realistic since the actuator

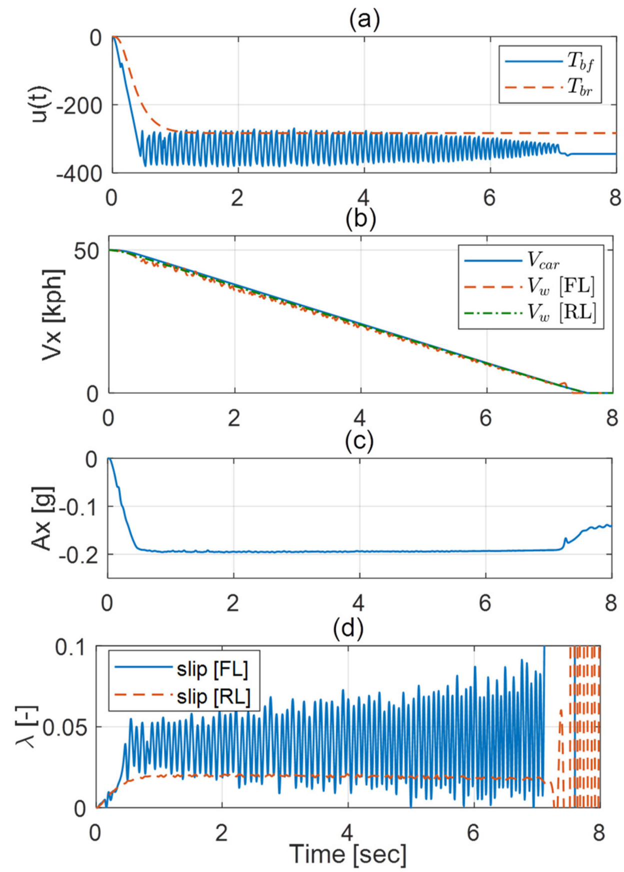

Fig. 7. Simulation results on a low friction road surface ($\mu = 0.20$) without actuation delay.

dynamics are not modeled. Therefore, very high frequency of wheel slip is observed, which can maximize the control performance.

We next present the results in Fig. 8 when the practical aspects of the actuators such as the bandwidth, pure time delay, and slew rate were considered to describe the actual experimental environment. These actuator dynamics may decrease the control performance, but the results are more realistic. Fig. 8 illustrates the results when the road surface transition occurs. This test is performed to verify robustness of the proposed method against surface environmental changes. The vehicle begins to decelerate at the surface of $\mu = 0.4$, and road friction is reduced to $\mu = 0.2$ around $t = 2$ sec. As shown in Fig. 8(a), the relatively large brake torques are applied when the vehicle is at the surface of $\mu = 0.4$ compared with that of Fig. 7(a), but the magnitude of the absolute value of brake torques decrease from $t = 2$ sec, which means that the algorithm can adapt to the new driving conditions. The controlled wheels are unstable shortly when surface transition occurs, but the designed controller stabilizes the vehicle immediately, as described in Fig. 8(b) and (d). The control performance can also be confirmed from the vehicle deceleration profile in Fig. 8(c).

In addition to the verified scenarios, the proposed method is effective even if the vehicle decelerates on the surface of split-mu where the left and right wheels have the different optimal

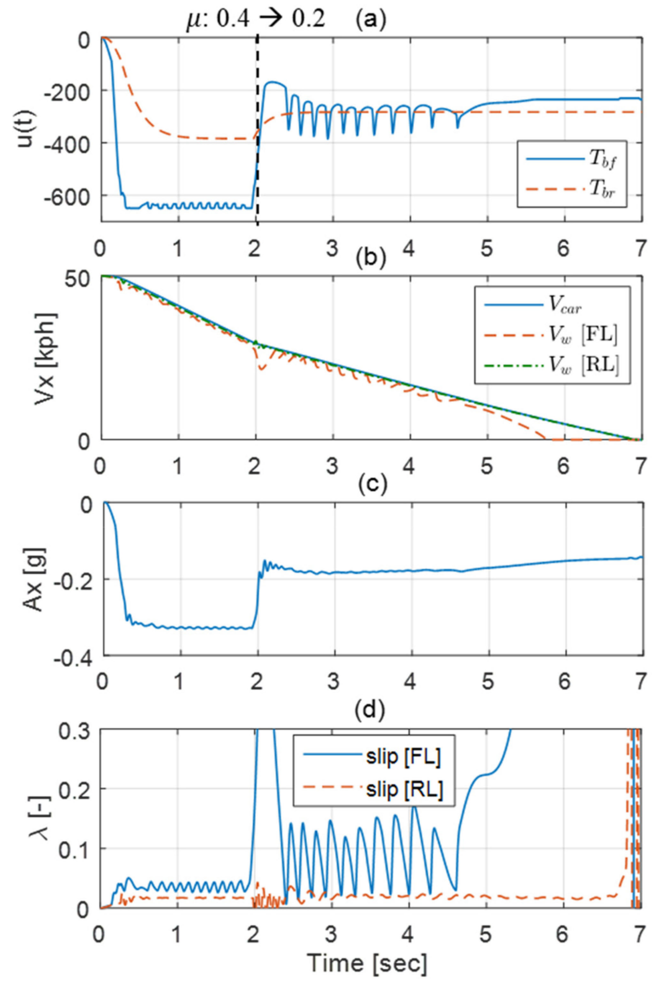

Fig. 8. Simulation results when the road surface transition occurs ($\mu = 0.40 \rightarrow 0.20$) with actuation delay.

slip points. The designed controller can detect the split-mu by monitoring the estimated individual tire force in (10), and both IWMs at the front wheels follow the wheel motion where a smaller road friction is detected. For example, if the road friction of the left wheel is 0.4 and the road friction of the right wheel is 0.2, the surface is considered as the homogeneous surface with $\mu = 0.2$.

Although the effectiveness of the algorithm in this simulation environment is demonstrated, the practical issues of actual driving that are not explicitly included in the simulation should be further investigated. Therefore, in the next section, we verify the robustness of the algorithm for these aspects through real vehicle-based experiments.

V. Experimental Results

A. Experimental Setup

The experiments were performed using a test vehicle on a proving ground. Photo of a vehicle is given in the Appendix, and the specifications of the vehicle model are summarized in Table III, see Appendix. To monitor the actual vehicle state

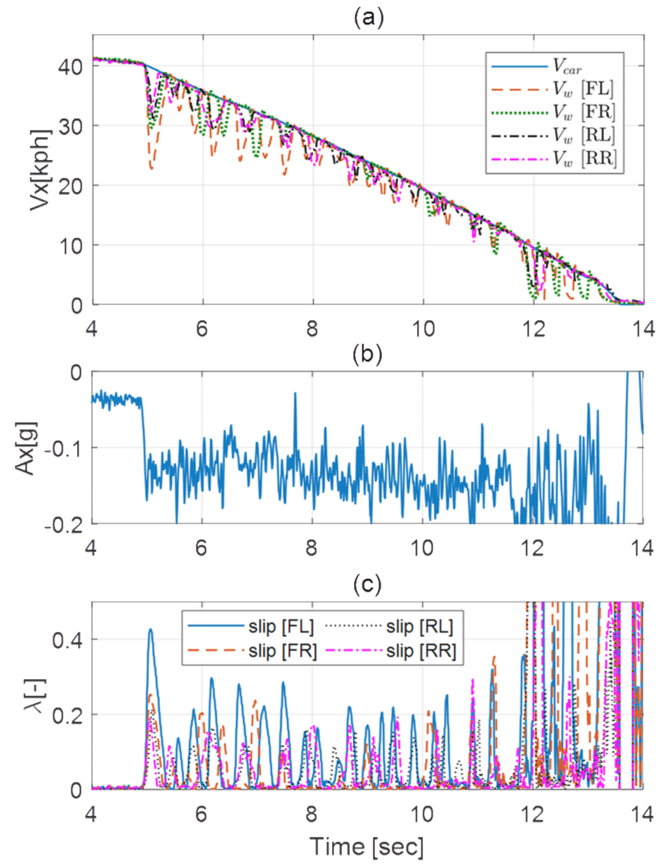

Fig. 9. Experimental results on wet tile surface using rule-based ABS.

variables, an RT-3100 device that is an accurate GNSS-aided inertial navigation system was installed inside the vehicle. Also, the sensor signals required for the proposed algorithm were obtained through a CAN bus monitoring system. The experiments were conducted on two types of road surface: a wet tile surface with $\mu \in [0.2, 0.3]$ and a Basalt surface with $\mu \in [0.3, 0.4]$.

B. Results

As shown in Figs. 9 and 10, the performance of the rule-based ABS controller that is implemented on the production vehicles was first verified for comparison purposes. Although the detailed control algorithm of this benchmarked could not be revealed due to the security reason, the mixed deceleration and slip control method, i.e., rule-based control, might be implemented on the test vehicle.

Fig. 9(a) describes the speed profile of the vehicle and wheels on the wet tile surface. The individual wheels were controlled by a conventional hydraulic brake system. It should be noted that all four wheels oscillated significantly to prevent locking up of the wheels, based on certain rules. As a result, Fig. 9(b) exhibits a wide range of changes in vehicle deceleration, which causes poor ride quality.

In addition, the large variations in individual wheel slip are observed in Fig. 9(c). Although the vehicle did not lose stability due to the rule-based ABS controller, individual tire stayed at optimum slip point for only a few seconds, which increases

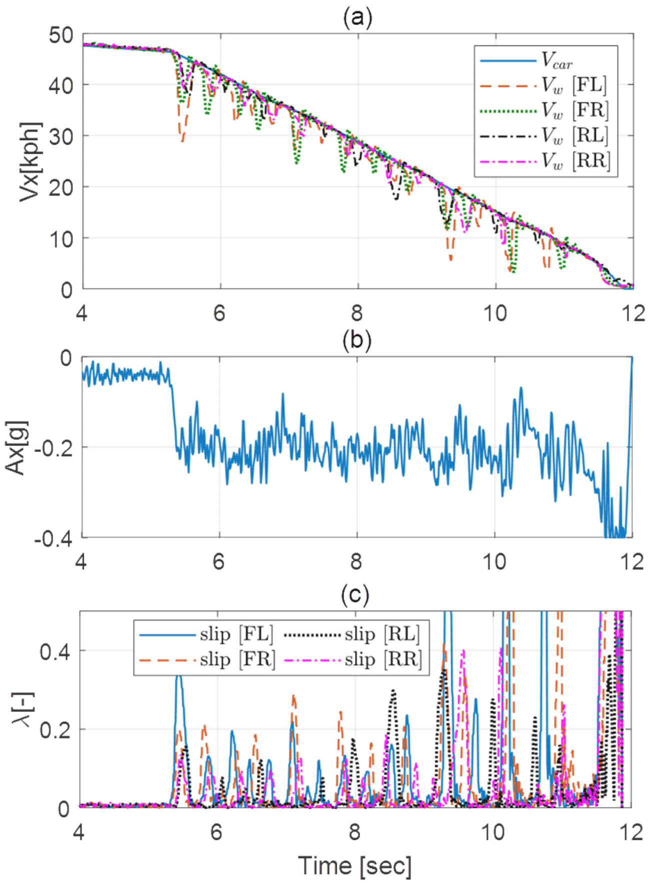

Fig. 10. Experimental results on Basalt surface using rule-based ABS.

the braking distance. It should be noted that braking distance is inversely proportional to average vehicle deceleration. In all experimental scenarios, it is not possible to repeat exactly the same experiment to compare the braking distances according to different controls, so we utilize the average vehicle deceleration as a performance index for a fair comparison.

Fig. 10 shows the performance of the conventional ABS using the same test vehicle on a Basalt road surface. Since the road friction increased a little, the test vehicle could decelerate slightly more than that in Fig. 9(b), as illustrated in Fig. 10(b). However, as shown in Fig. 10(a), a large deviation of the wheel speed from the vehicle speed similar to the previous test is still observed, which means that there is plenty of room for improvement in the control performance of the conventional ABS. The possibility of improved control performance can also be seen from the wheel slip profile, as illustrated in Fig. 10(c).

The performance of the proposed method is shown in Figs. 11 and 12. The tests are performed using the same vehicle on the same road surfaces. Fig. 11 shows the performance of the proposed algorithm on the wet tile surface. As expected, the IWMs at the front wheels are controlled to be cycled near the optimal wheel slip, as depicted in Fig. 11(a). Correspondingly, the hydraulic brake torque in Fig. 11(b) is applied to the rear wheels without large oscillations, and this brake torque is estimated from (5). Therefore, as illustrated in Fig. 11(c) and (e), only the front wheels are cycled to find the desired wheel speed, and the rear wheels maintain an almost constant wheel slip by tracking the desired wheel speed. This is quite distinguished compared to the results for the conventional ABS tested on the same surface in Fig. 9. As a result, a better ride quality is ensured, as shown in Fig. 11(d).

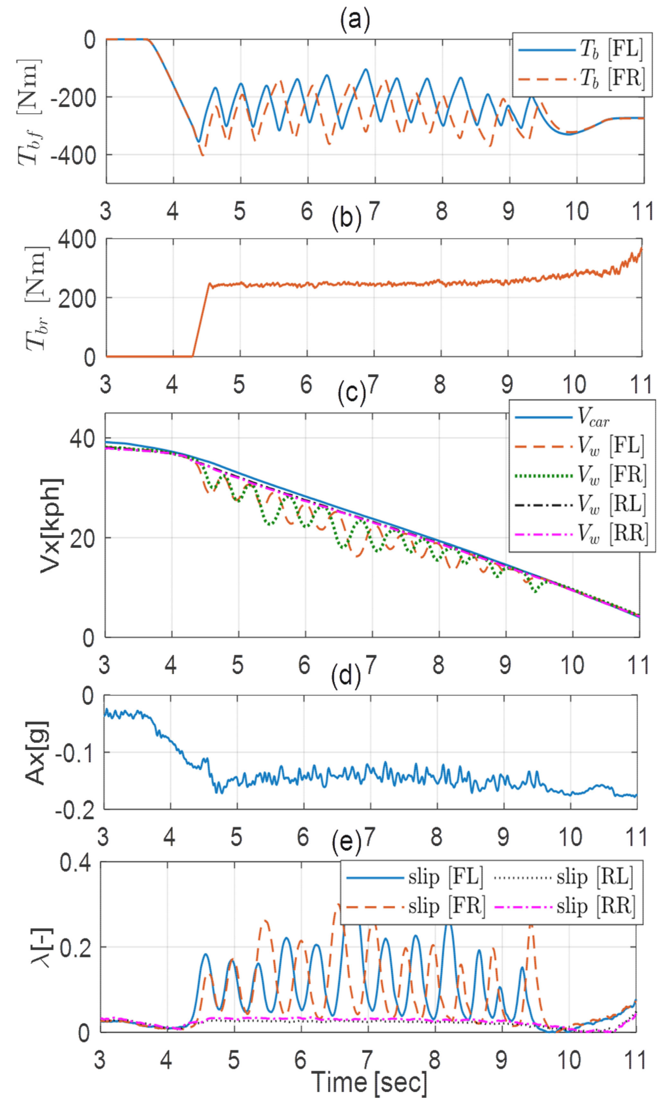

Fig. 11. Experimental results on wet tile surface using proposed method.

It should be noted that the IWMs employed in the test vehicle were not made for ABS control. Therefore, the hardware specifications such as time delay and sampling frequency are less than satisfactory level for wheel slip control. Although the deceleration performance is slightly improved compared to the results for the conventional ABS, more significant improvements of control performance are anticipated if the IWMs with faster dynamic characteristics is employed. In this verification, unfortunately, the IWMs significantly oscillated due to limited actuator performance, so the IWMs stayed on the desired wheel slip in a very short time. In addition, the controller is designed to give more control effort to the front wheels than to the rear wheels since the front wheels play an important role during braking because of the weight distribution of the vehicles. This

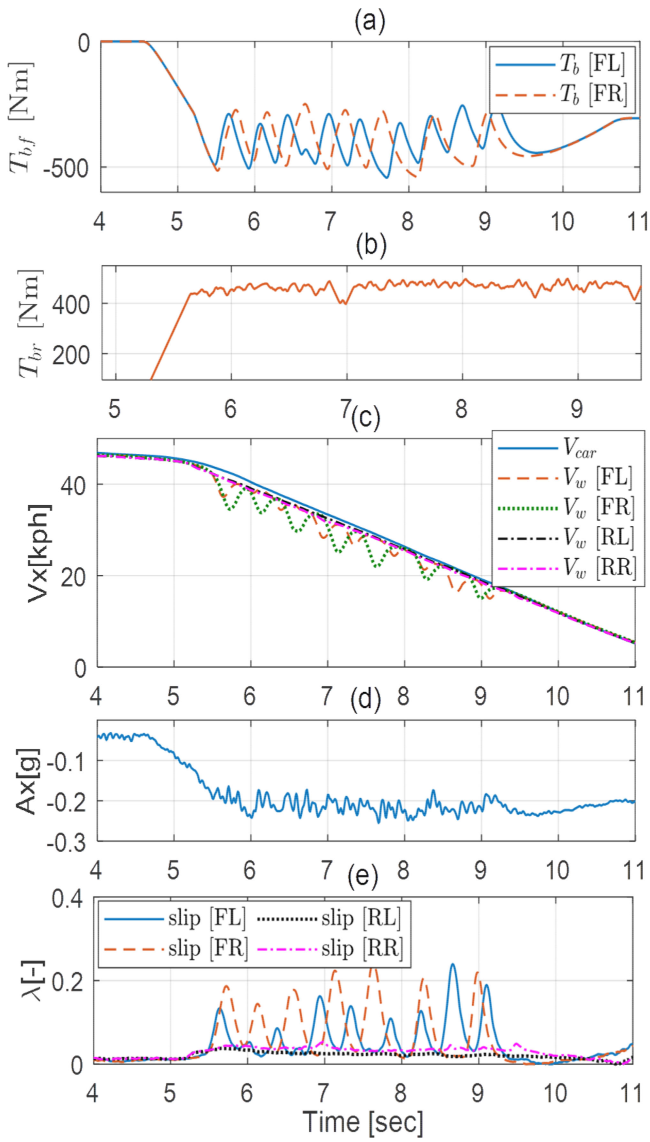

Fig. 12. Experimental results on Basalt surface using proposed method.

adjustment has been achieved by tuning the parameters ξ and ω_{rd}, and we have found that the active control of the front wheels and the under-actuation of the rear wheels provide the optimum solution for our target vehicle models. That is, the maximum average deceleration with the reduced the average jerk is observed with the current sets of ξ and ω_{rd}. However, the optimal solution depends on the vehicle and tire models, so the above-adjustment can be tuned empirically according to the model parameters. Also, from the results of the test we could verify that the actuators at each wheel faithfully fulfill their roles.

Lastly, the performance of the proposed method is validated on a Basalt surface, as depicted in Fig. 12, and results are very similar to those of the previous test. As the road friction increases, the motor torques in Fig. 12(a) also increase compared to that of Fig. 11(a). Accordingly, the applied rear brake torque of Fig. 12(b) is larger than that of Fig. 11(b). As a result, a small departure of the rear wheel speed in Fig. 12(c) results in small changes in vehicle deceleration in Fig. 12(d). In addition, the wheel slip profile of Fig. 12(e) is similar to that of Fig. 11(e).

TABLE II
COMPARISON OF AVERAGE DECELERATION AND JERK

Parameter	Quantity	Value
m	Gross vehicle weight (2UP)	2280 kg
l_f	Distance between the front axle and center of gravity	1.5 m
l_r	Distance between the rear axle and center of gravity	1.51 m
R	Effective wheel radius	0.335 m
J_w	Spin inertia for each wheel	0.9 kg $\cdot$ m^2
h	Height of center of gravity	0.55 m
t	Track width	1.6 m

In common with the above case, an IWM with a faster dynamic response can be employed to significantly reduce the large departure of the front wheel speeds. However, the hardware specifications could not be changed, and hence this could not be verified by experiments. However, by improving the hardware specifications in the simulation environment, reduced departure of the front wheel speed was confirmed, as presented in Section IV.

The CAN bus system runs with a sampling time of 10ms, but shorter update time is typically available for ABS control system. Usually, a sampling time of 7∼8 ms is utilized for conventional ABS controller. This shorter update time is possible because the hydraulic valves of conventional ABS are controlled by independent microprocessor rather than CAN bus system. Therefore, if the IWMs operate with independent motor controller rather than CAN bus system, more rapid dynamic response is expected.

Based on the several simulations, we can quantitatively determine the required dynamic response of IWM for the test vehicle to achieve the satisfactory control performance. For example, in the simulation verifications, we set a sampling time to 5 ms to increase the performance. In addition, a pure time delay for the IWM is recommended to be less than 10 ms.

Table II compares the control performance between the conventional method and the proposed method in terms of average vehicle deceleration and jerk. The higher magnitude of the average deceleration, the better the control performance. Moreover, a low average jerk is desirable for the ride quality. Based on these results, we can conclude that the proposed method can increase the control performance with the better ride quality. However, if the dynamic characteristics of IWM is improved in the future, the vehicle average deceleration can be further increased without any modification of the proposed approach.

VI. Conclusion

In this paper, a wheel slip-based ABS control algorithm is presented. Unlike the conventional method, the proposed method

(a) (b)

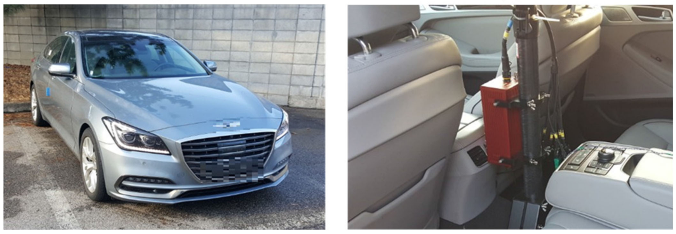

Fig. 13. (a) Test Vehicle (commercially available luxury sedan). (b) RT -3100 installed inside the vehicle.

can be realized without wheel slip and road friction information. This was possible by exploiting the nonlinear characteristics of tire force. In this way, we could find the optimal wheel slip at the front wheels using the fast-dynamics of the IWMs. Accordingly, the rear wheels are controlled to track the desired wheel speed by monitoring the cycling patterns of the front wheels. The proposed method is cost-competitive in that it only uses sensors that are measurable in production vehicles. The simulation and experiment confirm the feasibility of the proposed method and the proposed approach is expected to be applicable to any powertrain configuration (hybrid/electric vehicles and conventional hydraulic brake system). In addition, if actuators with better dynamic performance are employed in the future, a significant improvement in control performance is anticipated. Also, the vehicle lateral motion and split-mu surface should be further investigated to increase the possibility of mass production.

TABLE III
SPECIFICATION OF THE TEST VEHICLE MODEL

Cases \ Performance index		Deceleration $\lvert a_x \rvert$, (g)	Jerk $\lvert \dot{a}_x \rvert$, (g/s)
Wet tile surface (Figs. 9 and 11)	Conventional	0.137	1.272
	Proposed	0.146	0.3598
Basalt surface (Figs. 10 and 12)	Conventional	0.204	2.0
	Proposed	0.212	0.560

APPENDIX

Fig. 13(a) exhibits the test vehicle that is a commercially available. The IWMs are installed at the front wheels, and the torque for those can be controlled by the CAN protocol. Also, RT 3100 device is installed at the center of gravity for the purpose of measuring actual vehicle state variables, but unknown to the proposed algorithm, as depicted in Fig. 13(b).

REFERENCES

[1] A. T. Van Zanten, "Bosch ESP systems: 5 years of experience," SAE, Technical Paper 0148-7191, 2000, [Online]. Available: https://en.wikipedia.org/wiki/SAE_International

[2] J. Wang, L. Alexander, and R. Rajamani, "Friction estimation on highway vehicles using longitudinal measurements," *J. Dyn. Syst., Meas., Control*, vol. 126, no. 2, pp. 265–275, 2004.

[3] R. Rajamani, G. Phanomchoeng, D. Piyabongkarn, and J. Y. Lew, "Algorithms for real-time estimation of individual wheel tire-road friction coefficients," *IEEE/ASME Trans. Mechatronics*, vol. 17, no. 6, pp. 1183–1195, Dec. 2012.

[4] K. S. Han, E. Lee, M. Choi, and S. B. Choi, "Adaptive scheme for the real-time estimation of tire-road friction coefficient and vehicle velocity," *IEEE/ASME Trans. Mechatronics*, vol. 22, no. 4, pp. 1508–1518, Aug. 2017.

[5] M. Choi, J. J. Oh, and S. B. Choi, "Linearized recursive least squares methods for real-time identification of tire–road friction coefficient," *IEEE Trans. Veh. Technol.,* vol. 62, no. 7, pp. 2906–2918, Sep. 2013.

[6] J. J. Castillo, J. A. Cabrera, A. J. Guerra, and A. Simón, "A novel electrohydraulic brake system with tire–road friction estimation and continuous brake pressure control," *IEEE Trans. Ind. Electron.*, vol. 63, no. 3, pp. 1863–1875, Mar. 2016.

[7] Y.-H. J. Hsu, S. M. Laws, and J. C. Gerdes, "Estimation of tire slip angle and friction limits using steering torque," *IEEE Trans. Control Syst. Technol.*, vol. 18, no. 4, pp. 896–907, Jul. 2010.

[8] K. Han, M. Choi, and S. Choi, "Estimation of tire cornering stiffness as a road surface classification indicator using understeering characteristics," *IEEE Trans. Veh. Technol.*, vol. 67, no. 8, pp. 6851–6860, Aug. 2018.

[9] S. B. Choi, "Antilock brake system with a continuous wheel slip control to maximize the braking performance and the ride quality," *IEEE Trans. Control Syst. Technol.*, vol. 16, no. 5, pp. 996–1003, Sep. 2008.

[10] K. Han, M. Choi, B. Lee, and S. B. Choi, "Development of a traction control system using a special type of sliding mode controller for hybrid 4WD vehicles," *IEEE Trans. Veh. Technol.*, vol. 67, no. 1, pp. 264–274, Jan. 2018.

[11] D. Savitski, V. Ivanov, B. Shyrokau, T. Pütz, J. De Smet, and J. Theunissen, "Experimental investigations on continuous regenerative anti-lock braking system of full electric vehicle," *Int. J. Autom. Technol.*, vol. 17, no. 2, pp. 327–338, 2016.

[12] R. De Castro, R. E. Araújo, and D. Freitas, "Wheel slip control of EVs based on sliding mode technique with conditional integrators," *IEEE Trans. Ind. Electron.*, vol. 60, no. 8, pp. 3256–3271, Aug. 2013.

[13] Z. Wei and G. Xuexun, "An ABS control strategy for commercial vehicle," *IEEE/ASME Trans. Mechatronics*, vol. 20, no. 1, pp. 384–392, Feb. 2015.

[14] W.-Y. Wang, I.-H. Li, M.-C. Chen, S.-F. Su, and S.-B. Hsu, "Dynamic slip-ratio estimation and control of antilock braking systems using an observer-based direct adaptive fuzzy–neural controller," *IEEE Trans. Ind. Electron.*, vol. 56, no. 5, pp. 1746–1756, May 2009.

[15] S. Drakunov, U. Ozguner, P. Dix, and B. Ashrafi, "ABS control using optimum search via sliding modes," *IEEE Trans. Control Syst. Technol.*, vol. 3, no. 1, pp. 79–85, Jan. 1995.

[16] A. Dadashnialehi, A. Bab-Hadiashar, Z. Cao, and A. Kapoor, "Intelligent sensorless ABS for in-wheel electric vehicles," *IEEE Trans. Ind. Electron.*, vol. 61, no. 4, pp. 1957–1969, Apr. 2014.

[17] E. Dinçmen and T. Altınel, "An emergency braking controller based on extremum seeking with experimental implementation," *Int. J. Dyn. Control*, New York, NY, USA: Springer, vol. 6, no. 1, pp. 270–283, 2018.

[18] S.-I. Sakai, H. Sado, and Y. Hori, "Motion control in an electric vehicle with four independently driven in-wheel motors," *IEEE/ASME Trans. Mechatronics*, vol. 4, no. 1, pp. 9–16, Feb. 1999.

[19] K. Nam, Y. Hori, and C. Lee, "Wheel slip control for improving tractionability and energy efficiency of a personal electric vehicle," *Energies*, vol. 8, no. 7, pp. 6820–6840, 2015.

[20] H. Pacejka, *Tire and Vehicle Dynamics*. New York, NY, USA: Elsevier, 2005.

[21] V. Ivanov, D. Savitski, and B. Shyrokau, "A survey of traction control and antilock braking systems of full electric vehicles with individually controlled electric motors," *IEEE Trans. Veh. Technol.*, vol. 64, no. 9, pp. 3878–3896, Nov. 2015.

[22] S. Murata, "Innovation by in-wheel-motor drive unit," *Veh. Syst. Dyn.*, vol. 50, no. 6, pp. 807–830, 2012.

[23] R. Rajamani, G. Phanomchoeng, D. Piyabongkarn, and J. Y. Lew, "Algorithms for real-time estimation of individual wheel tire-road friction coefficients," *IEEE/ASME Trans. Mechatronics*, vol. 17, no. 6, pp. 1183–1195, Nov. 2012.

[24] K. Han, Y. Hwang, E. Lee, and S. Choi, "Robust estimation of maximum tire-road friction coefficient considering road surface irregularity," *Int. J. Autom. Technol.*, vol. 17, no. 3, pp. 415–425, 2016.

[25] H. K. Khalil and J. Grizzle, *Nonlinear Systems*. Englewood Cliffs, NJ, USA: Prentice-Hall, 1996.

[26] J. J. Oh, J. S. Eo, and S. B. Choi, “Torque observer-based control of self-energizing clutch actuator for dual clutch transmission,” *IEEE Trans. Control Syst. Technol.*, vol. 25, no. 5, pp. 1856–1864, Sep. 2016.

[27] Y. Shtessel, C. Edwards, L. Fridman, and A. Levant, *Sliding Mode Control and Observation*. New York, NY, USA: Springer, 2014.

[28] P. A. Ioannou and J. Sun, Adaptive Control. North Chelmsford, MA, USA: Courier Corporation, 2012.

Kyoungseok Han received the B.S. degree in civil engineering with a minor in mechanical engineering from Hanyang University, Seoul, South Korea, in 2013, and the M.S. and Ph.D. degrees in mechanical engineering from the Korea Advanced Institute of Science and Technology (KAIST), Daejeon, South Korea, in 2015 and 2018, respectively. He is currently a Postdoctoral Research Fellow at the University of Michigan, Ann Arbor, MI, USA. He mainly wrote this paper while working toward the Ph.D. degree with KAIST. His current research interests include vehicle dynamics and control, connected and automated vehicles technology, hybrid and electric vehicles, and optimization.

Byunghwan Lee received the B.S. and M.S. degrees in electronic, electrical, and computer engineering from Hanyang University, Seoul, South Korea, in 2011 and 2013, respectively. He is currently with the Hyundai-Kia R&D Center. His research interests include vehicle dynamics and hybrid electric vehicle control.

Seibum B. Choi (M’09) received the B.S. degree in mechanical engineering from Seoul National University, Seoul, South Korea, in 1985, the M.S. degree in mechanical engineering from the Korea Advanced Institute of Science and Technology (KAIST), Daejeon, South Korea, in 1987, and the Ph.D. degree in control from the University of California, Berkeley, CA, USA, in 1993. From 1993 to 1997, he was involved in the development of automated vehicle control systems at the Institute of Transportation Studies, University of California. During 2006, he was with TRW, Warren, MI, USA, where he was involved in the development of advanced vehicle control systems. Since 2006, he has been with the faculty of the Mechanical Engineering Department, KAIST. His current research interests include fuel-saving technology, vehicle dynamics and control, and active safety systems.